Chalcogenide Letters Vol. 14, No. 8, August 2017, p. 337 - 346

SYNTHESIS OF SILVER SULFIDE NANOPARTICLES THROUGH HOMOGENEOUS PRECIPITATION ROUTE AND THE PREPARATION OF THE Ag_2S-CHITOSAN NANOCOMPOSITES FOR THE REMOVAL OF IRON(II) ION FROM WASTEWATER

T. XABA[a*], M. J. MOLOTO[a], O. B. NCHOE[a], Z. NATE[a], N. MOLOTO[b]
[a]*Department of Chemistry, Vaal University of Technology, P/Bag X021, Vanderbijlpark, South Africa*
[b]*School of Chemistry, Wits University, P O Wits, Braamfontein, 2025, South Africa*

The simple synthesis of the Ag_2S nanoparticles through modified homogeneous precipitation route and the preparation of Ag_2S-chitosan nanocomposite is reported. The Ag_2S nanoparticles and the nanocomposites were characterized with ultraviolet–visible (UV-vis) spectroscopy, photoluminescence (PL), X-ray diffraction (XRD), transmission electron microscopy (TEM), and scanning electron microscope (SEM). The XRD pattern of the synthesized Ag_2S nanoparticles showed monoclinic crystal structure. TEM images of the nanoparticles and SEM micrograms of the nanocomposites revealed spherical shaped particles. Adsorption of Fe(II) ions from aqueous solution onto chitosan and Ag_2S-chitosan nanocomposites was studied in a batch system. The flame atomic absorption spectrophotometry (AAS) was used to analyse water samples. The effects of pH, and contact time were investigated. The results revealed that Ag_2S-chitosan nanocomposites can serves as better biosorbent as compared to purer chitosan.

(Received June 13, 2017; Accepted August 22, 2017)

Keywords: Silver sulfide nanoparticles, chitosan, nanocomposites, iron(II) ions, adsorption

1. Introduction

The scarcity of water and its quality due to the presence of heavy metals in our water streams is of great concern around the world. It has turn out to be a significant intimidation to the environment and human health. Recently, the toxicity of heavy metals and their removal from aqueous streams have attracted much attention [1-4]. Heavy metals such as lead, copper, zinc, iron, mercury, nickel etc. are usually discharged to the environment through several industrial activities such as electroplating, painting, smelting, mining, leather tanning, and battery engineering, etc., living a significant risk to the environment and human health [5].

Iron is one of the major impurities which is usually found in many water sources. The deposition of iron in the water distribution system may endorse the growth of microorganisms leading to high contamination in drinking water [6]. It is mainly existing in water in two forms either as soluble ferrous iron or insoluble ferric iron. Although iron is an important mineral that helps in the transportation of oxygen in the blood but if its occurrence to water systems is above a required level, it can makes water to be unusable due to its metallic taste discoloration, odour, and turbidity [7]. The high presence of iron in drinking water may cause vomiting, bleeding and circulatory disorders [8].

Numerous technologies and methods have been developed over the years to remove such materials from wastewater. Some of these technologies include flocculation/coagulation process [9], oxidation process [10, 11] etc. These technologies are generally expensive, time consuming and complicated to use. Due to the high cost of the present water treatment systems, most of the

*Corresponding author: thokozanix@vut.ac.za

developing countries are finding it hard to attain clean water and most of them are already drinking contaminated water. So, the introduction of a less expensive and easy preparative methods for water treatment system can be advantageous both socially and economically [12]. Adsorption process is regarded as the most effective technique among various methods available for water treatment, since it is more convenient and ease to operate [13].

Chitosan which is a second most plentiful natural biopolymer substance has been considered as a useful material for various purposes such as wastewater treatment, ion-exchanger and functional matrixes due to the highly reactive amino groups and carboxyl groups that are present in its matrix [14]. Chitosan has not only been used as an absorbent but it has also been utilized as a primary coagulant or flocculent due to its multi-functionality in the field of water and wastewater treatment applications [15–17]. Chitosan has protonated amines that form the multiple bonding sites that are useful in chelating with heavy metals.

Nanotechnology has been proven to be an effective route in solving water problems in our days [18]. Nanomaterials can invade deeper and thus can treat wastewater which is not possible with the other conventional methods [19]. The higher surface area-to-volume ratio of nanomaterials improves the reactivity of these materials with environmental contaminants. Among the nanomaterials, metal based nanomaterials have been confirmed to be better candidate in removing heavy metals than other nanomaterials such as activated carbon [20].

Silver sulfide nanomaterial is an important semiconductor material which has a direct band gap energy of 0.9 to 1.05 eV at normal temperature and has a quite large absorption coefficient. Ag_2S nanocrystals exhibit outstanding photoelectric properties [21–23]. These materials are broadly used in different fields such as solar cell batteries [24], thermoelectric sensors [25], photovoltaic cells, infrared detector, and superionic conductor [26-28]. Several physical and chemical methods have been reported for the synthesis of Ag_2S nanoparticles such as sol–gel method [29], micro-emulsion method [30], solvo-thermal method [31], and single source precursor routes [32]. But these techniques involve the use of toxic solvents and chemical substances which create a problem in the environmental. The utilization of green approach in the formation of nanomaterials have received significant attention recently since this part of chemistry deals with the rational design of products and processes which aims to reduce waste, prevent pollution, and to protect all living organisms [33].

The incorporation of silver sulfide nanoparticles with chitosan to form the polymer nanocomposite can synergistically improve the antimicrobial effect of the polymer. This combination can increase the surface charge of the composite and it can also multiply the number of bonding sites of the nanocomposite which will enable the heavy metals to be attracted easily on the surface of the nanocomposites. Despite the tremendous performance of chitosan based nonocomposites which is considered in many fields of adsorption, several reports based on silver chitosan nanocomposites have been investigated. However, to the best of our knowledge, the studies based on Ag_2S-chitosan nanocomposites for water treatment have never been reported before. Govindan et al. reported the synthesis and characterization of silver-chitosan nanocomposites through simple chemical reduction method. The chitosan based polymer nanocomposites exhibited good antimicrobial and antitumor properties [34]. The removal of Fe(II) and Zn(II) ions from aqueous solutions of chitosan via the batch system was reported by Hadi [35]. The adsorption studies proved that chitosan can be used as a biosorbent for the removal of heavy metals from waste water.

In this work, the synthesis of silver sulfide nanoparticles through simple, effective and eco-friendly modified homogeneous precipitation method is reported. The synthesized Ag_2S nanoparticles were then incorporated with chitosan to form polymer nanocomposites. The polymer nanocomposites were used to remove Fe^{2+} ions from the water sample using the batch experiment. The percentage removal efficiency was determined. The parameters such as changes in pH solution and the contact time during the experiment were investigated. The optical absorption, luminescence properties, and size distribution were characterized with UV-Vis and PL. The structural and morphological properties have been studied using XRD, TEM, and SEM. The flame atomic absorption spectrophotometry (AAS) was used to measure the concentrations of the solutions.

2. Experimental

2.1. Materials

Pyrrolidone, thiourea, silver acetate, chitosan, ammonium ferrous sulfate hexahydrate, methanol, and acetone were reagents from Sigma-Aldrich and were all used without further purification.

2.1.1. Synthesis of the silver sulfide nanoparticles.

The (Z)-2-(pyrrolidin-2-ylidene) thiourea ligand was prepared according to the procedure described previously [36] which is based on the reaction of pyrrolidone with thiourea. Ag_2S nanoparticles were synthesized by mixing silver acetate (5 mmol) in warm 50% methanol (20 mL) with (20 mL) warm 50% methanolic solution of the ligand (10 mmol) in a 100 mL two necked flask. The warm mixture was refluxed inside the water bath at 70 °C for an hour to produce a very dark solution. The synthesized Ag_2S nanoparticles were separated from the solution using centrifuge technique, washed with methanol and dried in an open air. Various instrumental techniques were used to characterize Ag_2S nanoparticles.

2.1.2. Preparation of Ag_2S*-chitosan nanocomposites.*

The synthesized Ag_2S nanoparticles (~3 mg) were dispersed in 10 mL of distilled water. The filtered nanoparticle solution was then transferred into a small beaker with 50 mL of 1% chitosan solution that was prepared from dilute acetic acid. The beaker with the mixture was then sealed with a foil and placed inside an ultra-sonic bath for 4 hrs to ensure the complete unification. The polymer nanocomposite mixture (5 mL) was transferred into a petri dish with a clean glass substrate which was previously washed with acetone. The solution inside the dish was allowed to evaporate inside the fume hood for 24 hrs to form the chitosan-Ag_2S nanocomposite films. The remaining Ag_2S nanocomposite solution was reserved for water treatment.

2.1.3. Batch adsorption experiments

A standard solution of 100 ppm of $(NH_4)_2Fe(SO_4)_2{\bullet}6H_2O$ was prepared as the stock solution. This solution was further diluted to certain concentrations ranging from 1 ppm to 50 ppm. Adsorption studies were conducted in batch mode at constant room temperature (25 ºC) to get optimum conditions such as pH and contact time. The studies were carried out using a 250 mL beaker containing 100 mL of 50 ppm Fe(II) ion stock solution. To study the effect of initial pH on the removal of Fe(II) ion, a 25 mL solution of Ag_2S-chitosan nanocomposites or 1% chitosan was added into a stock solution inside the beaker. The pH of a solution was varied from pH = 5 to pH = 11. The mixture was continually stirred using a magnetic stirrer for 1 hour. The pH of the solution was adjusted to different values with either 0.1 M NaOH or 0.1 M HCl. To study the effect of contact time, the same procedure as above was applied. The pH of a solution was adjusted to an optimum pH = 8. The study was carried out in a range of 0-3 hours. The solution was filtered using the filter paper during the entire processes and was taken for analysis.

2.2. Characterization

UV-1800 Shimadzu spectrophotometer and Gilden Fluorescence were used to measure the optical properties of Ag_2S nanoparticles and chitosan-Ag_2S nanocomposite films. The nanoparticles were dissolved in distilled water and solution was placed in a quartz cuvette with 1 cm path length. XRD patterns of the samples were obtained on a Phillips X'Pert chemistry research diffractometer using secondary monochromated Cu Kα radiation (λ = 1.54060 A°) at 40 Kv/30mA. Measurements were taken using a glancing angle of incidence detector at an angle of 2 for 2θ values over 10 to 80 in steps of 0.0167 with a scan speed of 0.0452. Transmission electron microscopy (TEM) was performed using a Tecnai F30 FEG TEM instrument at an accelerating voltage of 300 kV. TEM samples were prepared by placing 1 or 2 drop of Ag_2S nanoparticles dissolved in water/acetone mixture on lacey carbon copper grids. SEM analysis was performed using a Philips XL 30FEG. AAS analysis was made on the AA-7000 Shimadzu model coated GFA-7000 graphite furnace atomizer.

3. Results and discussion

3.1. Ag_2S nanocrystals and the deposition of Ag_2S polymer nanocomposite

The substituted thiourea ligand was used to synthesize silver sulfide nanoparticles through modified homogeneous precipitation route. The incorporation of Ag_2S nanoparticles into chitosan matrix to fabricate polymer nanocomposites using simple method has been investigated.

3.1.1.Optical properties

The peaks in the absorption spectra associated with the fundamental absorption edge of the samples can be used to predict the band gap of the nanomaterial [37]. Figure 1 shows the absorption spectrum, its corresponding Tauc plot and emission spectrum of the synthesized Ag_2S nanoparticles through homogeneous precipitation method. The measurements obtained in Fig. 1(a) (i) exhibited an absorption peak at 298 nm which is blue shifted from the bulk Ag_2S nanomaterial with the value of 620 nm (2.0 eV) [38].

The band gap can be projected by Tauc's relationship [39] between the optical absorption coefficient, α, the photon energy (hν), constant (*A*) and the direct band gap energy (Eg) as shown in eqn. (1) below:

$$\alpha h\nu = A(h\nu - E_g)^n \quad (1)$$

Where n = 0.5 for direct allowed transitions and n = 2 for indirect allowed transition. By plotting $(\alpha h\nu)^2$ against photon energy (hυ) and extrapolating the linear portion of the curve to absorption coefficient equal to zero, the Tauc plot in Fig. 1(a) (ii) reveals the estimated band gab of 4.27 eV. The blue shift in the band edge is a consequence of an exciton confinement and is also a confirmation of the presence of nanoparticulated materials. The results are in good agreement with those obtained previously [40-43].

The emission study based on the synthesis Ag_2S nanoparticles was done in order to investigate their luminescence properties. The emission spectrum of Ag_2S nanoparticles in Fig. 1(b) exhibit broad emission minima at 389 nm which is red-shifted with respect to the absorption edges. The strong band gap emission demonstrates the high crystalline nature of the synthesized nanoparticles. The broadening of the emission peak could be a consequence of the size distribution and the increase of the surface states could be due to high surface volume ratio for smaller particles [44].

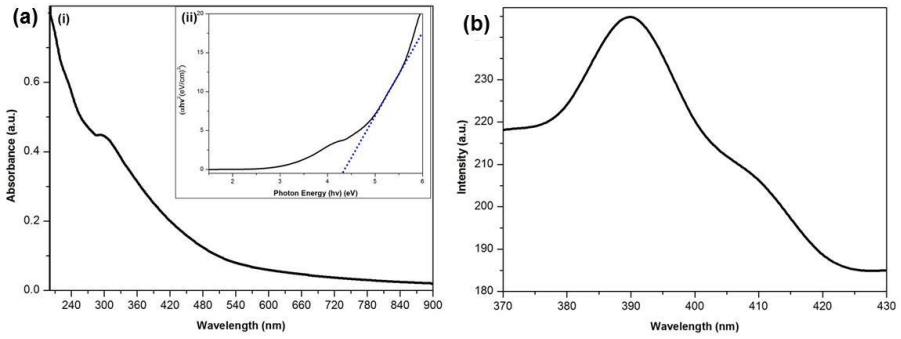

Fig. 1. Absorption & Tauc plot (a) and emission (b) spectra of Ag_2S nanoparticles

Fig. 2 shows the absorption and emission spectra of the chitosan and Ag_2S-chitosan nanocomposites. It is noted that when the Ag_2S nanoparticles are introduced into the surface of the chitosan, the absorption spectrum in Fig. 2(a) (ii) of Ag_2S-chitosan nanocomposites becomes red shifted compared to the spectrum of the pure chitosan (Fig. 2(a) (i)) with an absorption band edge at 516 nm (2.40 eV). The emission spectrum of the prepared Ag_2S-chitosan nanocomposites in Fig. 2(b) appeared to be broader which could be attributed to size distribution and the increase of the surface states due to the increase in surface area of the polymer and nanocomposites [45]. The

emission spectrum of pure chitosan in Fig. 2(b) (i) shows the emission maxima at 398 nm and a weak peak at around 474 nm, whereas the spectrum of the Ag_2S nanoparticles incorporated with chitosan is red shifted compared to the spectrum of the pure chitosan with two strong adjoining peaks at 399 and 421 nm in Fig. 2(b) (ii).

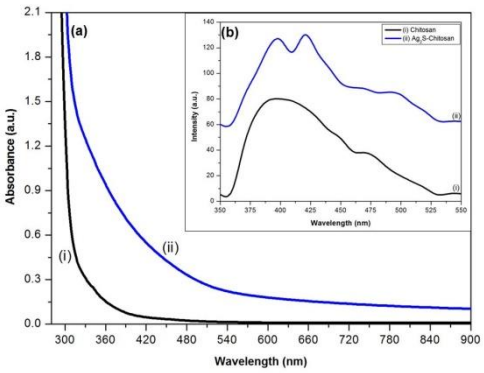

Fig. 2. Absorption (a) and emission (b) spectra of the chitosan and Ag_2S-chitosan nanocomposites

3.1.2. Structural properties

The p-X-ray diffraction patterns for the Ag_2S nanoparticles, chitosan, and Ag_2S-chitosan nanocomposites are shown in Fig. 3. Ag_2S nanoparticles in Figure 3(a) reveals relatively broad diffraction peaks diffraction peaks which is a good indication of the formation of small size particles. The XRD pattern was indexed to monoclinic crystal structure corresponding to the (110), (021), (111), (-112), (022), (112), (023), (-123), and (-114) planes of Ag_2S (acanthite, syn) which is in good agreement with the pattern JCPDS 00-014-0072. The obtained results are similar to those reported in the literature by Dong *et al*. and Lu *et al*. [42, 46].

The XRD pattern of the pure chitosan in Fig. 3(b) (i) exhibits diffraction peaks at 32.69°, a shoulder peak at 35.51°, 36.69°, 42.93°, and 80.66°. The Ag_2S-chitosan nanocomposites (Fig. 3(b) (ii)) revealed similar peaks as the diffraction pattern of the pure chitosan except that the shoulder peak at 35.51° in the XRD spectrum of the pure chitosan (Fig. 3(b) (i)) has disappeared from chitosan-Ag_2S nanocomposites spectrum.

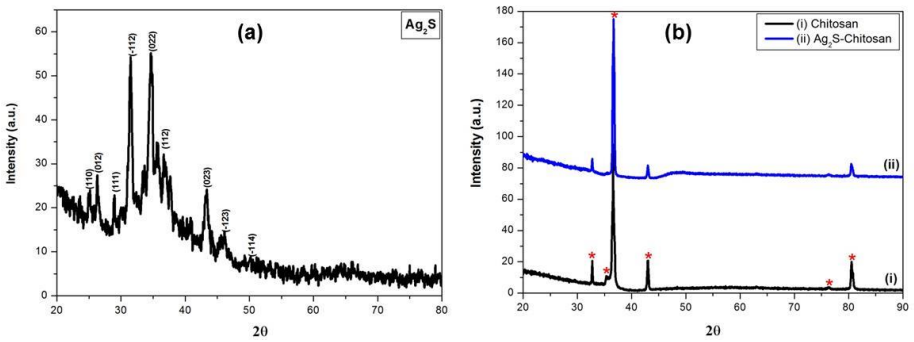

Fig. 3. X-ray diffraction patterns of Ag_2S nanoparticles (a) and chitosan & Ag_2S-chitosan nanocomposites (b)

The structural and morphological properties of Ag_2S nanoparticles, chitosan, and Ag_2S-chitosan nanocomposites are represented by Fig. 4. The morphological evaluation from TEM images of Ag_2S nanoparticles in Fig. 4(a) confirms monodispersed spherical shape particles. The corresponding size distribution histogram confirmed the average size of the particles of about 9.6 nm. The surface morphologies of the chitosan and Ag_2S-chitosan nanocomposites were analysed

using SEM technique. Fig. 4(b) shows SEM micrographs of Ag_2S nanocomposites which are nearly spherical in morphology together with big solid lumps which might be attributed to chitosan.

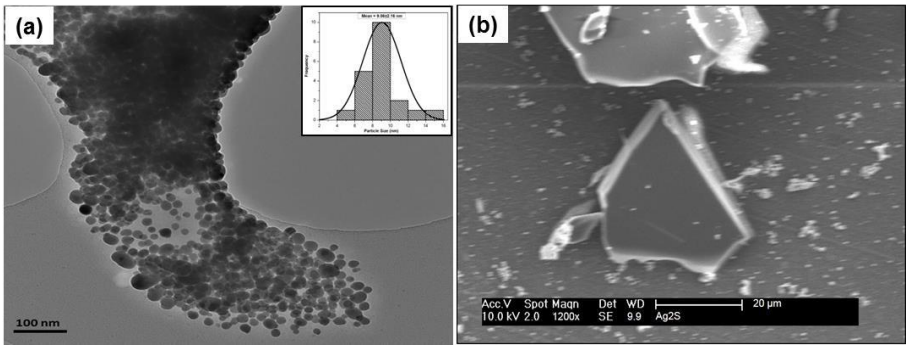

Fig. 4. TEM image of Ag_2S nanoparticles (a) and SEM micrograph of Ag_2S-chitosan nanocomposites (b)

3.2. Adsorption studies

Numerous factors affecting the removal of Fe(II) from waste water are investigated. The parameters such as pH, and contact time were studied using the batch experiment. After each filtration, the concentration of metal ions in supernatant was analysed using flame atomic absorption spectrophotometry (AAS). The amount of metal ion removed was calculated in percentage using the following formula (eqn. (2)):

$$\% \text{ Removal} = \frac{C_o - C_1}{C_o} \times 100\ \% \tag{2}$$

Where: C_o (ppm) is the initial metal ion concentration and C_1 (ppm) is the initial metal ion concentration and C_1 (ppm) is the final metal ion concentration in the solution

The study suggests that polymer nanocomposite such as Ag_2S-chitosan nanocomposites has a great influence in removing the heavy metal ion from waste water compared to the pure chitosan.

3.2.1. Effect of pH

The pH in adsorption studies plays an important role since it can influence the surface charge of the adsorbent by distributing the charge on the surface of an adsorbent between the adsorbate ions. The past studies have proven that at lower pH values, the binding sites of an adsorbent are generally protonated. Thus, repulsion occurs between the metal cation and the adsorbent. At higher pH values, the binding sites of the adsorbent start to deprotonate and generate different functional for metal binding [35]. Fig. 5 (a) & (b) shows that the pH influenced the removal efficiency of Fe(II) ions in the aqueous solution. The adsorption studies have proved that chitosan and chitosan nanocomposites adsorb metal cations mainly by chelation with amine groups [47, 48].

The results reveal that Fe(II) removal is increasing to maximum and then decreasing with pH variation from 5 to 11 at room temperature. The maximum % removal of Fe(II) ion from the solution was about 46% for pure chitosan solution in Fig. 5(a) and 67% for Ag_2S-chitosan nanocomposites in Fig. 5(b) at above neutral (pH = 8). These observations are similar to the results that were reported by Hadi [35]. When the pH was greater than 8 for both Fig. 5(a) & (b), Fe(II) ions started to precipitate as $Fe(OH)_2$. The increase in metal removal with an increase in pH can be clarified on the basis of the decrease in competition between proton and metal cations for same functional groups and by decrease in positive surface charge, which results in a lower electrostatic repulsion between surface and metal ions. Decrease in adsorption at higher pH (i.e. greater than pH = 8) is due to the formation of soluble hydroxy complexes [49].

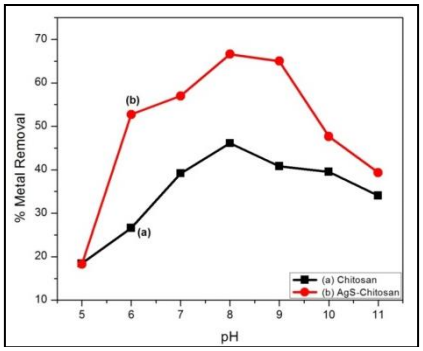

Fig. 5. Effect of pH on adsorption of Fe(II) ion using chitosan (a) and Ag_2S-chitosan nanocomposites (b) as absorbents

3.2.2. Effect of contact time

The contact time is one of the important factors that influence the adsorption process of heavy metals in a water treatment [50]. The effect of reaction time on Fe(II) ion adsorption process was determined by performing adsorption experiments at different contact time between the adsorbate (i.e. Fe(II) ion) and adsorbents(i.e. chitosan and Ag_2S–chitosan nanocomposites) in the range of 10–210 minutes at a pH of 8 and at room temperature. Fig. 6(a) & (b) shows that Fe(II) ions removal is increasing with an increase in contact time before equilibrium is reached. The results show the removal capacity of Fe(II) from 8 to 96% and from 19 to 99% using chitosan and Ag_2S–chitosan nanocomposites as absorbents. It has been noted that from 170-210 minutes, the percentage removal of Fe(II) remains constant, which showed that equilibrium was reached at 170 minutes by both absorbents which signif the optimum contact time for this type of absorbance. These results are very important since equilibrium time is one of the most important parameters for economical wastewater treatment systems.

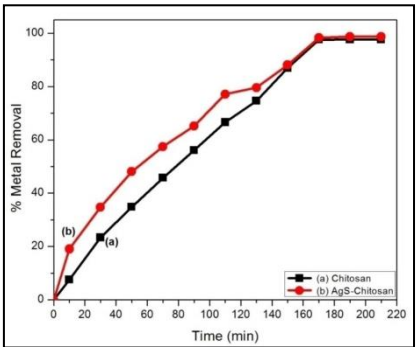

Fig. 6. Effect of contact time on adsorption of Fe (II) ion using chitosan (a) and Ag_2S–chitosan nanocomposites (b) as absorbents

3.2.3. Mechanism of heavy metal removal

The adsorption of heavy metals is strongly depending on the surface area and pore structure of the adsorbent [51]. The adsorption on chitosan and its nanocomposites mainly depends on amino and hydroxyl groups [52]. The surface area of these materials consist of numerous amino and hydroxyl groups that are sensible to bind with the metal ions. The lone pair on the nitrogen and oxygen atoms are presented to the empty atomic orbitals of the metal ion, which creates coordination complexes on the surface of the material [53]. Metal ions such as iron (II) ions coordinate in a square planar configuration [54] and the configuration of amino groups chelated with metal ions is called the bridge model [55]. Scheme 1 shows the mechanism in which the metal ions coordinate with the heavy metals during adsorption process.

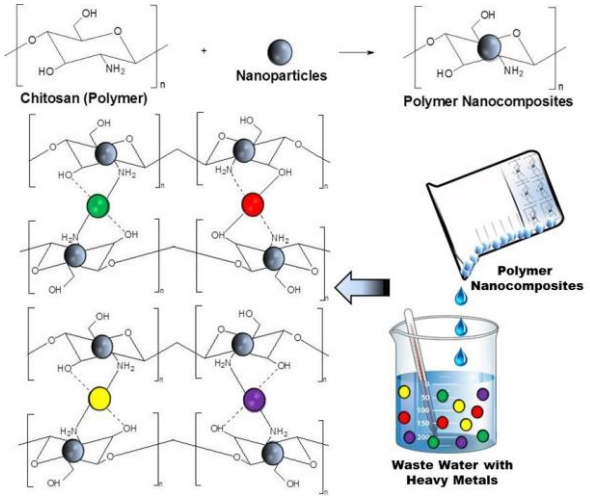

Scheme 1. The mechanism of the formation of nanocomposites and the adsorption of heavy metal on chitosan based nanocomposites

4. Conclusions

The synthesis of Ag_2S nanoparticles has been done through the homogeneous precipitation method from (Z)-2-(pyrrolidin-2-ylidene) thiourea ligand. The TEM images of Ag_2S nanoparticles showed well-dispersed spherical shaped particles. Chitosan based Ag_2S nanocomposite was prepared through a simple method. UV-Vis results of the prepared Ag_2S–chitosan nanocomposites showed the characteristics of both nanoparticles and polymer. The optical absorption results were blue shifted compared to that of the bulk materials. The SEM images proved that indeed the incorporation of the nanoparticles to the polymer was achieved. Batch adsorption studies for the removal of Fe(II) ions from aqueous solution have been carried out using pure chitosan and polymer nanocomposites.

The study shows that Fe(II) ions adsorption onto the adsorbents depends highly on the pH of the solution and the contact time. The optimum pH of the solution for the removal of iron(II) ions from the water sample using pure chitosan and chitosan nanocomposites as adsorbents was found to be 8 and the optimum reaction time for adsorption of iron(II) ions was found to be 170 min with the percentage removal efficiency of 99% and 96% from both adsorbents. The study also proved that Ag_2S–chitosan nanocomposites can be regarded as the best adsorbents compared to the pure chitosan since its results reveal the highest percentage removal of Fe(II) ion from the water sample.

Acknowledgements

The authors would like to acknowledge the Vaal University of Technology and National Research Foundation (TTK13071722088: “Thuthuka Grant Holder”)) for funding this project.

References

[1] M. Bhaumik, A. Maity, V. V. Srinivasu, M. S. Onyango, Chem Eng J. **181**, 323 (2012).
[2] R. Ansari, A. F. Delavar, J. Iran Chem. Soc. **5**, 657 (2008).
[3] R. Ansari, N. K. Fahim, A. F. Dellavar, J. Iran Chem. Res. **2**, 163 (2009).
[4] R. Ansari, Z. Mosayebzadeh, Reactive and Functional Poly. **67**, 367 (2007).
[5] O. Ozay, S. Ekici, Y. Baran, N. Aktas, N. Sahiner, Water Research **43**, 4403 (2009).
[6] J. D. Navratil, and M.T. S. Tsair, Water science and Technology **47**, 29 (2002).

[7] B. Das, P. Hazarika, G. Saikia, H. Kalita, D. C. Goswami, H. B. Das, S.N. Dube, R. K. Dutta, Journal of Hazardous materials. **141**, 834 (2007).
[8] Ryoma Bun- E1, N. Kawasaki, F. Ogata, T. Nakamura, K. Aochi, S. Tanada, Journal of oleo science. **55**, 423 (2006).
[9] O. S. Amuda. I. A. Amoo, O. O. Ajayi, J. Hazard. Mater. **129**, 69 (2006).
[10] N. S. S. Martinez, J. F. Fernandez, X. F. Segura, A. S. Ferrer, J. Haz. Mat. **B101**, 315 (2003).
[11] J. A. Peres, J. Beltran de Heredia, J. R. Dominguez, J. Haz. Mat. **107**, 115 (2004).
[12] N. Abdel-Raouf, A. A. Al-Homaidan, I. B. M. Ibraheem, Saudi journal of biological sciences. **19**, 257 (2012).
[13] A. Bhatnagar, M. Sillanpa, Chem Eng J. **157**, 277 (2010).
[14] G. Crini. Bioresour, Technol. **90**, 193 (2003).
[15] E. Assaad, A. Azzouz, D. Nistor, A.V. Ursu, T. Sajin, D.N. Miron, F. Monette, P. Niquette, R. Hausler, Appl. Clay Sci. **37**, 258 (2007).
[16] A. R. Cestari, E. F. S. Vieira, A. M. G. Tavares, R. E. Bruns, J. Hazard. Mater. **153**, 566 (2008).
[17] W.P. Cheng, F.H. Chi, R.F. Yu, Y.C. Lee, J. Polym. Environ. **13**, 383 (2005).
[18] W. Zhang, F. A. DiGiano, Water Research, **36**, 1469 (2002).
[19] P. Gautam, D. Madathil, A. N. Brijesh Nair, International Journal of ChemTech Research **5**, 2303 (2013).
[20] Y. C. Sharma, V. Srivastava, V. K. Singh, S. N. Kaul, C. H. Weng, Environmental Technology, **30**, 583 (2009).
[21] K. Nagasuna, T. Akita, M. Fujishima, H. Tada, Langmuir, **27**, 7294 (2011).
[22] M. Pang, J. Hu, H. C. Zeng, J. Am. Chem. Soc., **132**, 10771 (2010).
[23] Y. Du, B. Xu, T. Fu, M. Cai, F. Li, Y. Zhang, Q. Wang, J. Am. Chem., Soc. **132**, 1470 (2010).
[24] A. Tubtimtae, K. -L. Wu, H. -Y. Tung, M. -W. Lee, G. J. Wang, Electrochem. Commun. **12**, 1158 (2010).
[25] S. Yan, K. Shen, X. Xu, S. Yi, J. Wu, Z. Xiao, Synth. Met. **161**, 1646 (2011).
[26] M. C. Brelle, J. Z. Zhang, Chem J Phys **108**, 3119 (1998).
[27] D. Bruhwiler, C. Leigener, S. Glaus, G. Calzaferri, J Phys Chem B. **106**, 3770 (2002).
[28] S. Kitova, J. Eneva, A. Panov, H. Haefke, Imaging J Sci Fechnol. **38**, 484 (1994).
[29] J. P. Xiao, Y. Xie, R. Tang, W. Luo, J Mater Chem. **12**, 1148 (2002).
[30] J. C. Liu, P. Raveendran, Z. Shervani, Y. Ikushima, Chem Commun. **22**, 2582 (2004).
[31] C. Yu, M. Leng, M. Liu, Y. Yu, D. Liu, C. Wang, Cryst Eng Comm. **14**, 3772 (2012).
[32] T. G. Schaaff, A. J. Rodinone, J Phys Chem B. **107**, 10416 (2003).
[33] P. N. Joshi, Green Chemistry for Nanotechnology: Opportunities and Future Challenges, RRJCHEM, **5**, 1 (2016).
[34] S. Govindan, E. A. K. Nivethaa, R. Saravanan, V. Narayanan, A. Stephen, Appl Nanosci. **2**, 299 (2012).
[35] A. G. Hadi, International Journal of ChemTech Research. **9**, 343 (2016).
[36] T. Xaba, M. J. Moloto, N. Moloto, Materials Letters, **146**, 91 (2015).
[37] T. T. Q. Hoa, L. V. Vu, T. D. Canh, N. N. Long, J. Phys. **187**, 012081 (2009).
[38] N. Moloto, N. Revaprasadu, M. J. Moloto, P. O'Brien, J. N. Raftery, S. Afr. J. Sci. **105**, 258 (2009).
[39] J. Tauc, R. Grigorovici, A. Vancu, Phys. Status Solidi. **15**, 627 (1966).
[40] M. Liu, Z. Xu, B. Li, C. Lin, D. Bai, N. Shan, W. You, Mater. Lett. **65**, 555 (2011).
[41] M. Wu, X. Pan, X. Qian, J. Yin, Z. Zhu, Inorg. Chem. Commun. **7**, 359 (2004)
[42] L. Dong, Y. Chu, Y. Liu, L. Li, J. Colloid Interface Sci. **317**, 485 (2008).
[43] M. Kristl, S. Gyergyek, J. Kristl, Mater. Express. **5**, 359 (2015)
[44] S. Biswas, S. Kar, Nanotechnology. **19**, (2008) 045710.
[45] D. C. Onwudiwe, P. A. Ajibade, Int. J. Mol. Sci. **12**, 5538 (2011).
[46] Q. Lu, F. Gao, D. Zhao, Angew Chem Int Ed. **41**, 1932 (2002).
[47] J. Dai, F. L. Ren, C. Y. Tao. Molecules. **17**, 4388 (2012).
[48] R. Graciela, S. Jorge, A. F. Jaime, Purif. Technol. **44**, 31 (2005).

[49] R. R. Devi, I. M. Umlong, B. Das, K. Borah, A. J. Thakur, P. K. Raul, S. Banerjee, L. Singh, Applied Water Science. **4**, 175 (2014).
[50] T. Akar, S. Tunali, Minerals Engineering. **18**, 1099 (2005).
[51] B. Kuchta, L. Firlej, G. Maurin, J. Mol. Model. **11**, 293 (2005).
[52] K. Yu, J. Ho, E. McCandlish, B. Buckley, R. Patel, Z. Li, N. C. Shapley, Colloids Surf. A. **425**, 31 (2013).
[53] C. M. Futalan, C. -C. Kan, M. L. Dalida, C. Pascua, M. -W. Wan, Carbohydr. Polym. **83**, 697 (2011).
[54] S. Z. Bajwa, P. A. Lieberzeit, Sens. Actuators B. **207**, 976 (2015).
[55] O. A. C. Monteiro, C. Airoldi, J. Colloid Interface Sci. **212**, 212 (1999).